On combining temperature and pressure effects on structural properties of crystals with standard ab initio techniques.

A. Erba
On combining temperature and pressure effects on structural properties of crystals with standard ab initio techniques.
THE JOURNAL OF CHEMICAL PHYSICS (2014) 141

On Combining Temperature and Pressure Effects on Structural Properties of Crystals with Standard Ab initio Techniques.

A. Erba[1, a)]
Dipartimento di Chimica and Centre of Excellence NIS (Nanostructured Interfaces and Surfaces), Università di Torino, via Giuria 5, IT-10125 Torino (Italy)

(Dated: 9 September 2014)

A general-purpose, fully-automated, computationally-efficient implementation is presented of a series of techniques for the simultaneous description of pressure and temperature effects on structural properties of materials, by means of standard *ab initio* simulations. Equilibrium volume, bulk modulus, thermal expansion coefficient, equation-of-state, Grüneisen parameter, constant-pressure and constant-volume specific heats are computed as a function of temperature and pressure for the simple crystal of diamond and compared with accurate experimental data. Convergence of computed properties with respect to super-cell size is critically discussed. The effect on such properties of the adopted exchange-correlation functional of the density-functional-theory is discussed by considering three different levels of approximation (including hybrids): it is found to be rather small for the temperature dependence of equilibrium volume and bulk modulus, whereas it is quite large as regards their absolute values.

I. INTRODUCTION

Standard *ab initio* quantum-chemical methods based on the Density Functional Theory (DFT) represent a powerful tool for the accurate determination of a variety of properties of materials (structural, electronic, vibrational, optical, elastic, magnetic, etc.).[1–4] The increasing efficiency of the algorithms and the growing parallel computing resources are rapidly widening the range of applicability of such schemes which can now be routinely used for studying minerals of geophysical interest, defective materials for the electronics, adsorption of biomolecules on biomaterials, porous materials for hydrogen storage, etc.[5–8] Such methods, however, describe the ground state of the system at zero temperature and pressure which is a severe limitation to their general applicability. The effect of pressure, for instance, is particularly relevant to the study of minerals at geophysical conditions[9] while temperature is affecting a large variety of properties (also simple ones such as equilibrium structure and electron charge distribution), even at ambient conditions.[10,11]

The effect of pressure on structural properties of materials can be accounted for in a relatively simple way either by fitting energy-volume data to a given analytical expression for the equation-of-state (EOS),[12–16] or by performing pressure-constrained geometry optimizations where cell gradients are corrected for by the proper hydrostatic stress term.[17,18] Pressure can also be included into elastic response properties;[19–22] the algorithm for the elastic tensor calculation has recently been generalized to include such effect in the public Crystal program, for instance.[23,24]

Modeling the effects of temperature is a much more difficult task. Despite the entrance into a new age of molecular quantum chemistry has recently been declared ("*In the fourth age we are able to incorporate into our quantum chemical treatment the motion of nuclei [...] and compute accurate, temperature-dependent, effective properties, thus closing the gap between measurements and electronic structure computations*"),[25] we are still far from having such schemes efficiently implemented, in particular for the solid state. The most effective technique for taking into account temperature effects (including anharmonic terms) on computed properties of materials, in particular as regards thermal nuclear motion, would be *ab initio* molecular dynamics which, however, is still rather computationally demanding.[26–28]

Two main features have to be modeled in order to properly account for the effect of temperature on materials: i) volume expansion, and ii) nuclear motion. The two effects are obviously physically interconnected but, with standard *ab initio* methods, require quite different techniques to be properly described so that it proves convenient to treat them separately. Most structural properties of materials are dominated by thermal expansion which requires the determination of the equilibrium volume at different temperatures, $V(T)$; an explicit account of lattice dynamics is then needed, even for predicting zero temperature properties by including zero-point motion (ZPM) effects, commonly neglected, which may significantly affect equilibrium volume and bulk modulus determinations. Due to the fact that core and inner-valence electrons of atoms follow the movement of the respective nuclei, when electron charge density (ECD) and related X-ray structure factors are considered, it is mandatory to account for the effect of thermal nuclear motion, for instance by means of atomic Debye-Waller factors.[29–31] An enormous amount of literature has been devoted to the approximate evaluation of such effects in order to allow for a correct interpretation of the X-ray scattering data.[11] It has recently been shown that very accurate directional Compton profiles, as measured from the inelastic scattering of high intensity synchrotron radiation by single-crystal samples,[32,33] can reveal subtle

a) Electronic mail: alessandro.erba@unito.it

aspects of the electron momentum distribution (EMD) of periodic systems.[34–37] At variance with ECD, nuclear motion effects on the EMD of a crystal are extremely subtle and can be predicted with either *ad hoc* models[38,39] or rather sophisticated *ab initio* techniques.[40]

In the present work, a general-purpose, fully-automated, computationally-efficient implementation is presented of an *ab initio* theoretical scheme for the combined inclusion of temperature and pressure effects on structural properties of materials. All the implemented algorithms can be executed in parallel and massive-parallel mode, up to several thousands of CPUs, with a high scaling.[41,42]

Within the frame of standard quantum chemical methods, temperature can be modeled by explicitly treating the lattice dynamics. To do so, a harmonic approximation (HA) to the lattice potential is commonly adopted which proved extremely effective in predicting vibration properties of a variety of materials, when light atoms such as H, He and Li are absent. Drawbacks of the HA are well-known; among others, zero thermal expansion.[43,44] The simplest way of going beyond the HA, without explicitly computing phonon-phonon interaction coefficients, is represented by the so-called quasiharmonic approximation (QHA) which introduces the missing volume dependence of phonon frequencies by retaining the harmonic expression for the Helmholtz free energy.[45,46]

According to the QHA, the equilibrium volume, $V(T)$, at any temperature T can then be deduced by minimizing Helmholtz's free energy $F(V;T)$. This approach also allows for the natural combination of temperature and pressure effects: the equilibrium structure at any temperature and pressure can be computed. Depending on the temperature and pressure ranges to be explored, the lattice dynamics has to be solved at few volumes in the expansion and compression regime, respectively. Within such a formal scheme, a simplified model (namely, Grüneisen approach) has been extensively used in the past according to which a linear dependence of phonon frequencies on volume in the vicinity of the equilibrium is assumed.[10] Let me stress that, generally (and particularly so when small cell systems are studied), within the direct-space approach to phonon calculation, supercells have to be considered in order to make the lattice dynamical description converge.

Both schemes are here implemented into a development version of the public CRYSTAL14 program for quantum-chemistry and -physics of the solid state, which adopts one-electron Hamiltonians and atom-centered Gaussian-type function basis sets.[42,47] The implemented algorithms are applied to the simple case of diamond, whose thermal expansion has been accurately characterized both experimentally[48–50] and theoretically.[51–56]

The structure of the paper is as follows: the main formal aspects of harmonic lattice dynamics and quasi-harmonic approximation are introduced in Section II; details about the implemented algorithm are given in Section III; preliminary results on diamond are presented and discussed, with respect to available experimental and theoretical data, in Section IV where the effect of the adopted one-electron Hamiltonian is illustrated into some detail; conclusions are drawn in Section V.

II. THEORETICAL FRAMEWORK

The formalism of harmonic lattice dynamics is briefly recalled in Section II A in order to fix the notation. The main limitations of the harmonic approximation, in particular as regards the zero thermal expansivity, are mentioned in Section II B where the principal aspects of the simplest approach for going beyond it, namely quasi-harmonic approximation, are presented.

A. Elements of Harmonic Lattice Dynamics

Within the Born-Oppenheimer approximation, the quantum-mechanical description of nuclear motions is dictated by the shape of the potential energy surface $E(\mathcal{R})$. The configuration $\mathcal{R}$ which describes the instantaneous position of all nuclei in the crystal can be specified by assigning to each of them the displacement with respect to the equilibrium position: $\mathcal{R} \equiv \{\dots\ ,\ [(\mathbf{R}_0)_a + \mathbf{g} + \mathbf{x}_a^{\mathbf{g}}]\ ,\ \dots\}$. The index a ($a = 1, \dots, N$) labels the general nucleus in the unit cell and $(\mathbf{R}_0)_a$ is its equilibrium position in the reference zero cell; the lattice vector $\mathbf{g} = \sum_{m=1}^{3} l_m^g\, \mathbf{a}_m$ identifies the general crystal cell where $\mathbf{a}_m$ are the direct lattice vectors. In a cyclic crystal model, the integers l_m^g run from 0 to $L_m - 1$. When dealing with cubic crystals (as here for simplicity) all L_m's are set to a common value L. The parameter L defines the size of a supercell (SC).

The potential field $E(\mathcal{R})$ is a function of the displacements $\mathbf{x}_a^{\mathbf{g}}$ or, equivalently, of their Cartesian coordinates $x_j^{\mathbf{g}}$, the index j running from 1 to $3N$. In what follows, matrix notation is used; uppercase letters in bold and lowercase letters in bold with over-line represent $3N \times 3N$ matrices and $3N$ vectors, respectively. Thus, the Cartesian coordinates of the displacements are represented by vectors $\overline{\mathbf{x}}^{\mathbf{g}}$. By expanding $E(\mathcal{R})$ in a Taylor series with respect to these coordinates about the equilibrium $\mathcal{R}_0$ configuration, after setting $E(\mathcal{R}_0) = 0$, and exploiting translational invariance, one gets:

$$E(\mathcal{R}) = \frac{L^3}{2} \sum_{\mathbf{g}} \left(\overline{\mathbf{x}}^{\mathbf{0}}\right)^T \mathbf{V}^{\mathbf{g}} \overline{\mathbf{x}}^{\mathbf{g}} + \mathcal{O}_3(\{\overline{\mathbf{x}}^{\mathbf{g}}\})\ , \qquad (1)$$

where L^3 Hessian matrices $\{\mathbf{V}^{\mathbf{g}}\}$ have been introduced whose elements are defined as $\mathbf{V}^{\mathbf{g}}_{ai,bj} = \partial^2 E/(\partial x^{\mathbf{0}}_{ai} \partial x^{\mathbf{g}}_{bj})$ and are energy second derivatives with respect to the displacement of atom a along the i-th Cartesian direction in the reference $\mathbf{0}$ cell and atom b along the j-th Cartesian direction in the $\mathbf{g}$ crystal cell.

The *harmonic approximation* (HA) to the lattice potential consists in neglecting all $\mathcal{O}_3$ terms in equation

(1). On the one hand, the HA has experienced an enormous success in the study of vibration properties of crystals due not only to its simplicity but also to its predicting power. Standard solid state quantum-mechanical programs, based on one-electron Hamiltonians, can accurately and efficiently evaluate the second-order energy derivatives with respect to atomic displacements. When suitable Hamiltonians are adopted (like the popular hybrid B3LYP functional), an extremely accurate description of vibrational phonon frequencies can be achieved for most crystalline compounds, as long as very light atoms (such as H, He, Li) are not considered.[57–59] On the other hand, the HA has a large number of significant deficiencies that will be mentioned in Section II B.

Translational invariance allows for the factorization of the harmonic nuclear Schrödinger equation into L^3 separate ones, each associated with a wavevector $\mathbf{k} = \sum_{n=1}^{3} (\kappa_n/L)\, \mathbf{b}_n$ where $\mathbf{b}_n$ are the reciprocal lattice vectors and the integers κ_n run from 0 to $L-1$. For each $\mathbf{k}$, the *dynamical matrix* $\mathbf{W^k}$ is defined as Fourier transform of the Hessian matrices $\{\mathbf{V^g}\}$:[21]

$$\mathbf{W^k} = \sum_{\mathbf{g}=1}^{L^3} \mathbf{M}^{-\frac{1}{2}} \mathbf{V^g} \mathbf{M}^{-\frac{1}{2}} \exp(\imath \mathbf{k} \cdot \mathbf{g}) \,, \tag{2}$$

where $\mathbf{M}$ is the diagonal matrix of the nuclear masses. The solution is obtained by diagonalizing the dynamical matrices $\left\{\mathbf{W^k}\right\}$:

$$(\mathbf{U^k})^\dagger \, \mathbf{W^k} \, \mathbf{U^k} \;=\; \mathbf{\Lambda^k} \,. \tag{3}$$

$3N$ phonons, labeled by a band index j ($j = 1, \ldots, 3N$), are associated with each of the L^3 $\mathbf{k}$-points, whose frequencies $\omega_{\mathbf{k}j}$ are related to the eigenvalues $\lambda_{\mathbf{k}j}$ via $\omega_{\mathbf{k}j} = 2\pi\sqrt{\lambda_{\mathbf{k}j}}$. The columns of the $\mathbf{U^k}$ matrix in equation (3) represent the corresponding normal mode coordinates.

B. Quasi-Harmonic Approximation

When the lattice dynamics of a crystal is solved within the purely HA, vibration frequencies are described as independent of interatomic distances and the corresponding vibrational contribution to the internal energy of the crystal turns out to be independent of volume. It follows that, within such an assumption, a variety of physical properties would be wrongly described: thermal expansion would be null, elastic constants would not depend on temperature, constant-pressure and constant-volume specific heats would coincide with each other, thermal conductivity would be infinite as well as phonon lifetimes, etc.[43,44]

An explicit account of anharmonic effects would require the calculation of phonon-phonon interaction coefficients with techniques (such as Vibrational Configuration Interaction, VCI, Vibrational Self-Consistent-Field, VSCF, Vibrational Perturbation Theory, VPT, Transition Optimized Shifted Hermite, TOSH, calculation of higher order interatomic force constants, etc.) that are rather computationally demanding for large systems.[60–64] A simple and powerful approach for correcting most of the above mentioned deficiencies of the HA is the QHA.[45]

According to the QHA, the Helmholtz free energy, F, of a crystal is written retaining the same harmonic expression[65] but introducing an explicit dependence of vibration frequencies on volume:[45,46]

$$F^{\mathrm{QHA}}(T,V) = U_0(V) + F^{\mathrm{QHA}}_{\mathrm{vib}}(T,V) \,, \tag{4}$$

where $U_0(V)$ is the zero-temperature internal energy of the crystal without any vibrational contribution (a quantity commonly accessible to standard *ab initio* simulations) and the vibrational part reads:

$$F^{\mathrm{QHA}}_{\mathrm{vib}}(T,V) = E_0^{\mathrm{ZP}}(V) + k_B T \sum_{\mathbf{k}j} \left[\ln\left(1 - e^{-\frac{\hbar\omega_{\mathbf{k}j}(V)}{k_B T}} \right) \right] \,, \tag{5}$$

where k_B is Boltzmann's constant, $\hbar$ Planck's constant, $\omega_{\mathbf{k}j}(V)$ the volume-dependent vibration frequency of the j-th phonon of reciprocal point $\mathbf{k}$ and $E_0^{\mathrm{ZP}}(V) = \sum_{\mathbf{k}j} \hbar\omega_{\mathbf{k}j}(V)/2$ is the zero-point energy of the system. The zero-pressure equilibrium volume at a given temperature T, $V(T)$, is obtained by minimizing $F^{\mathrm{QHA}}(V;T)$ with respect to volume V and keeping T as a fixed parameter. From the volume-temperature relation $V(T)$, the volumetric thermal expansion coefficient $\alpha_V(T)$ is obtained as:

$$\alpha_V(T) = \frac{1}{V(T)} \left(\frac{\partial V(T)}{\partial T} \right)_{P=0} \,. \tag{6}$$

For cubic crystals, a linear thermal expansion coefficient $\alpha_l(T)$ is commonly considered which is simply $\alpha_l(T) = \alpha_V(T)/3$. The temperature-dependent bulk modulus, $K(T)$, can be obtained as an isothermal second derivative of equation (4) with respect to the volume:

$$K(T) = V(T) \left(\frac{\partial^2 F^{\mathrm{QHA}}(V;T)}{\partial V^2} \right)_T \,. \tag{7}$$

By differentiating equation (4) with respect to the volume and changing sign, one gets the pressure-volume relation, at a given temperature:

$$P(V;T) = -\frac{\partial F^{\mathrm{QHA}}(V;T)}{\partial V} = -\frac{\partial U_0(V)}{\partial V} - \frac{\partial F^{\mathrm{QHA}}_{\mathrm{vib}}(V;T)}{\partial V} \,. \tag{8}$$

By numerically inverting the above expression, the volume-pressure relation at any given temperature, $V(P;T)$, is derived which can be used to define the volumetric thermal expansion coefficient at any pressure P as:

$$\alpha_V(T;P) = \frac{1}{V(T;P)} \left(\frac{\partial V(T;P)}{\partial T} \right)_P \,. \tag{9}$$

The mean vibrational energy of a phonon (*i.e.* harmonic oscillator) with angular frequency $\omega_{\mathbf{k}j}(V_0)$, in thermal equilibrium at temperature T, is given by:

$$\mathcal{E}[\omega_{\mathbf{k}j}(V_0)] = \hbar\omega_{\mathbf{k}j}(V_0)\left[\frac{1}{2} + \frac{1}{e^{\frac{\hbar\omega_{\mathbf{k}j}(V_0)}{k_B T}} - 1}\right] . \quad (10)$$

By differentiating with respect to temperature the sum over all possible phonons of $\mathcal{E}[\omega_{\mathbf{k}j}(V_0)]$, one obtains an expression for the constant-volume specific heat of the crystal, $C_V(T)$:

$$C_V(T) = \sum_{\mathbf{k}j} \frac{\partial \mathcal{E}[\omega_{\mathbf{k}j}(V_0)]}{\partial T} = \sum_{\mathbf{k}j} C_{V,\mathbf{k}j}(T) \quad (11)$$

$$= \sum_{\mathbf{k}j} \frac{[\hbar\omega_{\mathbf{k}j}(V_0)]^2}{k_B T^2} \frac{e^{\frac{\hbar\omega_{\mathbf{k}j}(V_0)}{k_B T}}}{\left(e^{\frac{\hbar\omega_{\mathbf{k}j}(V_0)}{k_B T}} - 1\right)^2} , \quad (12)$$

where a mode contribution, $C_{V,\mathbf{k}j}$, to the specific heat has been introduced. The difference between constant-pressure and constant-volume specific heats can be expressed in terms of quantities defined above as:[21]

$$C_P(T) - C_V(T) = \alpha_V^2(T) K(T) V(T) T . \quad (13)$$

1. Grüneisen Approach

Grüneisen formalism assumes a linear dependence of vibration phonon frequencies on volume, in the vicinity of the zero temperature equilibrium volume V_0.[10] The key quantity is here represented by the dimensionless mode Grüneisen parameter which proved to be particularly useful in the fundamental understanding of the mechanism of thermal expansion of crystals; for each phonon, it reads:

$$\gamma_{\mathbf{k}j} = -\frac{V_0}{\omega_{\mathbf{k}j}(V_0)} \left(\frac{\partial \omega_{\mathbf{k}j}(V)}{\partial V}\right)_{V=V_0} . \quad (14)$$

An overall thermal Grüneisen parameter, $\gamma(T)$ can be defined as the weighted average of the various mode Grüneisen parameters in terms of the corresponding mode contribution to the specific heat, which proves useful in reducing high-temperature equations-of-state into shock-compression experiments:[66]

$$\gamma(T) = \sum_{\mathbf{k}j} \frac{\gamma_{\mathbf{k}j}\, C_{V,\mathbf{k}j}(T)}{C_{V,\mathbf{k}j}(T)} . \quad (15)$$

Within Grüneisen approach, the volumetric thermal expansion is given by:

$$\alpha_V^{\mathrm{gru}}(T) = \frac{1}{K V_0} \sum_{\mathbf{k}j} \gamma_{\mathbf{k}j}\, C_{V,\mathbf{k}j}(T) . \quad (16)$$

III. COMPUTATIONAL PROCEDURE

The general-purpose, fully-automated algorithm, as implemented in a development version of the public CRYSTAL14 program, for computing the properties introduced in Section II B is here illustrated. The asymmetric unit of the starting crystalline structure, defined according to the space group it belongs to, is first fully-optimized by use of analytical energy gradients with respect to both atomic coordinates and unit-cell parameters,[67–69] with a quasi-Newtonian technique combined with the Broyden-Fletcher-Goldfarb-Shanno algorithm for Hessian updating.[70–73] Convergence is checked on both gradient components and nuclear displacements. Once the zero temperature, zero pressure equilibrium volume V_0 has been determined (zero-point motion effects are neglected at this stage), an explored volume range is defined where the most compressed volume is $V_c = x_c V_0$ and the most expanded volume is $V_e = x_e V_0$, with $0 < x_c < 1$ and $x_e > 1$. The width of the adopted volume range has to be set depending on the values of pressure and temperature to be explored. A number N_V of equidistant volumes, including V_0, is considered within this range.

For each considered volume V_i ($i = 1, \ldots, N_V$), a full volume-constrained geometry optimization is performed. Phonon frequencies $\{\omega_{\mathbf{k}j}(V_i)\}$ are then computed according to the formalism described in Section II A (more details on the implementation of phonon calculation with CRYSTAL can be found in Refs. 74 and 75); the energy second derivatives defining the Hessian matrices $\{\mathbf{V^g}\}$ are computed as numerical first derivatives of analytical gradients by displacing all and only symmetry-independent atoms along symmetry-independent Cartesian directions. From computed phonon frequencies, thermodynamic properties are evaluated, at almost zero computational cost, at N_T equidistant temperatures T_t in the range $T_1 \leq T_t \leq T_2$: $\{F^{\mathrm{QHA}}(T_t; V_i)\}$ ($t = 1, \ldots, N_T$), for instance, from equation (5).

When all volumes $\{V_i\}$ have been considered, internal energy/volume data, $\{U_0(V_i)\}$, are fitted to various equations-of-state (the third-order Murnaghan's,[12] third-order Birch's,[13,14] logarithmic Poirier-Tarantola's,[15] and exponential Vinet's[16]) to determine the zero temperature bulk modulus K_0, still without zero-point motion effects, according to the methodology recently implemented in CRYSTAL.[23] It is worth mentioning that, in order to perform numerically the derivative of equation (14) for computing mode Grüneisen parameters, the continuity of phonon frequencies among different volumes has to be established: scalar products of the corresponding normal modes are performed for resolving possible crossings.

Let me stress that, apart from the definition of the temperature and pressure ranges to be explored (which can be modified at almost zero computational cost by means of complete restart calculations, see case i) below), the only parameters to be specified as an input to the entire procedure are x_c, x_e and N_V, defining range

TABLE I. Equilibrium volume of the primitive cell, V_0, and bulk modulus, K_0, of diamond at zero pressure and temperature, as computed with different Hamiltonians and compared with experimental values.[50,76] Data in parentheses are obtained by neglecting ZPM effects. The lattice parameter is given by $a_0 = (4V_0)^{1/3}$.

	LDA	PBE	B3LYP	Exp.
V_0	11.11	11.49	11.48	11.34
	(10.99)	(11.36)	(11.35)	
K_0	467.5	431.2	439.5	442.1
	(476.8)	(441.5)	(449.2)	

and number of the explored volumes. The whole algorithm then reduces to a single-run calculation due to its fully-automated feature. In the present study, $x_c = 0.98$ (corresponding to a 2 % compression) and $x_e = 1.04$ (corresponding to a 4 % expansion). The number of explored volumes is $N_V = 5$. Computed results are not changed by using a larger number of volumes in this case.

Three distinct levels are available for the restart option: i) a restart from a previous complete calculation that can be used to explore different ranges of temperature and pressure at almost zero computational cost; ii) a restart from a previous incomplete calculation where only the first m geometry optimizations and phonon calculations were performed; iii) a restart from a previous incomplete calculation where m geometry optimizations and $m-1$ phonon calculations were performed.

In order to make all the thermodynamical properties converge, super-cells (SC) calculations have to be generally performed, unless the primitive cell of the system is already large enough. The SC size is proportional to the parameter L introduced in Section II A; its effect on computed properties will be discussed in Section IV. The implemented algorithms can be executed in parallel and massive-parallel mode, up to several thousands of CPUs, with a high scaling, as recently demonstrated in Refs. 41 and 42.

IV. RESULTS AND DISCUSSION

When standard *ab initio* quantum-mechanical techniques are applied, equilibrium structural properties of materials at zero temperature are usually determined by neglecting ZPM effects. Merits and limitations of different one-electron Hamiltonians are often discussed by comparing computed values with the outcomes of low-temperature experimental measurements. The ZPM effect is commonly neglected in that its proper account would require the explicit description of the lattice dynamics which is a computationally much more demanding task than simple static geometry optimizations.

ZPM effects on structural properties of diamond are shown in Table I where equilibrium volume of the primitive cell, V_0, and bulk modulus, K_0, at zero pressure and temperature are reported, as computed with different functionals of the DFT (a local-density approximation, LDA, the Perdew-Burke-Ernzerhof generalized-gradient functional, PBE,[77] and the popular B3LYP hybrid functional[78,79] with 20 % of exact Hartree-Fock exchange). All-electron atom-centered Gaussian-type function basis sets of triple-zeta valence quality, augmented by a polarization function (namely, TZVP), are adopted.[80] Experimental values from low-temperature measurements are also reported: V_0 determined at 4.2 K with the X-ray diffraction Bond method on a high-purity single crystal of synthetic diamond[50] and K_0 from Brillouin scattering measurements,[76] as reported in Ref 81. The static values (in parentheses), without ZPM effects, are obtained by fitting electronic energy-volume data to the third-order Birch-Murnaghan equation of state.[13,14] It is seen that, by neglecting ZPM, an excellent agreement could be claimed for the PBE functional on both volume and bulk modulus; a very similar, slightly better, agreement would be obtained with the B3LYP hybrid functional for V_0 only. When the ZPM is included in the calculations, V_0 increases by about 1 % and K_0 decreases by about 2.3 %. If PBE and B3LYP still give essentially the same description of V_0, the values they provide for K_0 are quite different from each other. The PBE error (just 0.1 % without ZPM) increases to 2.6 % by including ZPM. Correspondingly, B3LYP decreases from 1.6 % down to 0.6 %. Then, B3LYP appears to provide the best description of these two properties for diamond. The ZPM effect is even larger for another simple cubic crystal as MgO where V_0 is increased by 2 % and K_0 decreased by 6 %.[66]

The results to be presented in this section depend on a few computational parameters. In particular, their convergence with respect to the number of **k**-points (see equation 5 for Helmholtz free energy and 11 for constant-volume specific heat, for instance) has to be carefully checked. Equivalently, within the direct space SC approach that is used here, convergence must be checked with respect to the size of the adopted SC (see the L parameter introduced in Section II A). Different thermodynamical quantities usually converge with different speeds, entropy being generally somehow slower than specific heat.

In Figure 1, the constant-pressure specific heat of diamond $C_P(T)$ is reported as a function of temperature, as computed at the PBE level with equation (13). Experimental data from Refs. 82 and 83 are also shown for comparison. The total computed $C_P(T)$ is reported (solid line) as obtained from the largest SC considered in this study: a conventional cubic cell with $L = 5$, containing a total of 1000 carbon atoms (namely, C5); a massive-parallel implementation of all the algorithms involved has

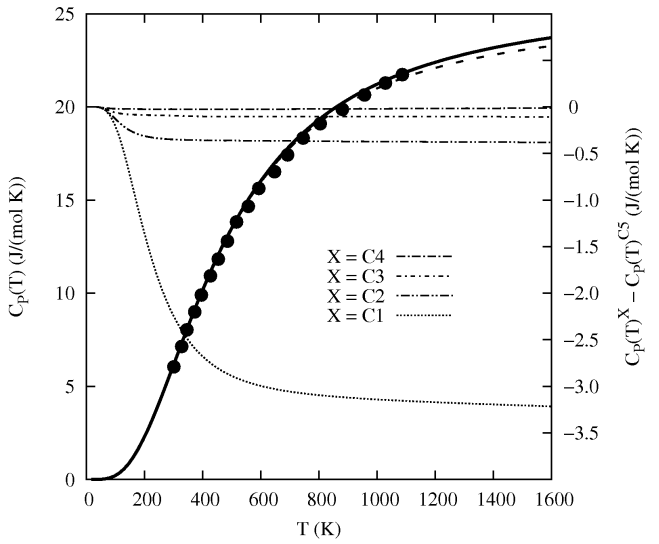

FIG. 1. Constant-pressure specific heat of diamond as a function of temperature. Circles are experimental data at room pressure from Refs. 82 and 83, as reported in Ref. 52. The solid line corresponds to the computed specific heat with the largest SC explored, namely a C5 SC (see text for details); the dashed curve is the corresponding constant-volume specific heat. On the right-hand side scale, the effect of the SC size is shown: differences of the specific heat computed with SCs of increasing size and that obtained with the largest one are reported. All computed data are obtained with the PBE functional.

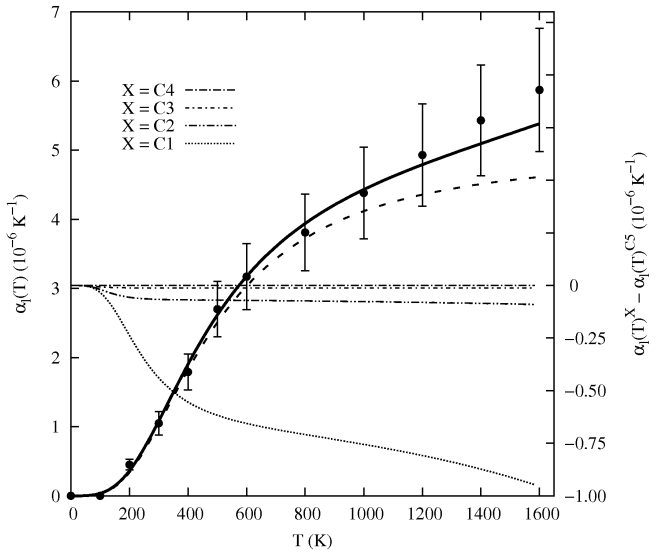

FIG. 2. Linear thermal expansion coefficient for diamond as a function of temperature. Experimental data at room pressure by Slack and Bartram[48] are reported with the corresponding error-bars. The continuous line represents computed values obtained with the Helmholtz free energy approach; dashed line represents computed values from the Grüneisen approach. On the right-hand side scale, the effect of the SC size is shown: differences of the linear expansion coefficient computed with SCs of increasing size and that obtained with the largest one, C5, are reported for the Helmholtz free energy approach. All computed data are obtained with the PBE functional.

been used in order to run such a large calculation.[42] The agreement with the experiment is shown to be rather good. The dashed line in the figure represents the constant-volume specific heat $C_V(T)$ as computed with the same SC. The difference $C_P(T) - C_V(T)$ is relatively small, increases as a function of temperature and becomes non-negligible above 1000 K. In the same figure (right-hand side scale), the effect of the SC size is also explored. Differences are reported between the specific heat computed with conventional SCs of increasing size (one with $L = 1$ containing 8 atoms, C1, one with $L = 2$ containing 64 atoms, C2, one with $L = 3$ containing 216 atoms, C3 and one with $L = 4$ containing 512 atoms, C4) and that obtained with the largest one, C5.[84] It is seen that the specific heat provided by the C1 SC is 13 % far from C5 at 1600 K. A conventional cell containing 64 atoms, C2, already assures a convergence within 2 % and constitutes the smallest model that one could reliably use for studying thermodynamical properties of diamond. The C3 SC is only 0.4 % apart from the limit at 1600 K while C4 coincides with C5.

The main quantity to be computed in order to describe the effect of temperature on structural properties of materials is the thermal expansion coefficient $\alpha(T)$. In Figure 2, the linear expansion $\alpha_l(T)$ of diamond is reported as a function of temperature, as measured by Slack and Bartram[48] (full circles; the corresponding error-bars are also given) and as computed at PBE level with the largest SC, C5, with both a Grüneisen approach (dashed line) and a Helmholtz free energy approach (continuous line). It is seen that the descriptions given by the two approaches almost coincide at low-temperatures and then deviate from each other above room temperature; at 1600 K, the difference is as large as 10 %. The theoretical description given by Helmholtz's approach is well within the experimental error bars. The computed $\alpha_l(T)$ is found to be slightly larger than experiment at about 800 K and a bit smaller above 1200 K. A very similar behavior has also been reported by Mounet and Marzari, in 2005, in their PBE density-functional perturbation theory study,[52] and by Herrero and Ramírez in their path-integral Monte Carlo study, in 2000, which explicitly included also anharmonic effects.[55] Previous theoretical determinations of the thermal expansion of diamond, both using the Grüneisen and Helmholtz approaches, provided lower values for $\alpha_l(T)$ thus confirming the inadequacy of the former approach at high-temperatures and showing a possible incompleteness of the lattice dynamical description in the latter.[51,53]

On the right-hand side scale of Figure 2, the effect of the SC size is shown on $\alpha_l(T)$, as computed by minimizing Helmholtz free energy. Differences of the linear expansion coefficient computed with SCs of increasing size and that obtained with the largest one, C5, are reported.

As already observed for the specific-heat of Figure 1, also in this case the C2 SC provides results which are almost converged, still 2 % apart from the limit. C3 is 0.2 % apart and convergence is fully reached with C4. In this respect, let me anticipate some of the evidences to be reported soon in a couple of forthcoming studies on the thermal expansion of a family of alkali halides (LiF, NaCl, KCl, NaF, KF, LiCl, LiBr, KBr, NaBr) and simple oxides (MgO and CaO). All these crystals contains 2 atoms in their primitive cells. In all cases, thermal expansion properties are found to be perfectly converged with SCs containing just 16 atoms, which makes such calculations definitely affordable as regards their computational cost. The case is a bit different (*i.e.* larger SCs have to be considered) if absolute thermodynamical properties, such as entropy, specific heat and Helmholtz free energy, have to be converged.

The effect of the adopted one-electron Hamiltonian on computed zero-temperature structural properties, such as V_0 and K_0, has already been shown in Table I; the LDA and PBE determinations of V_0 differ by 3.6 % and those of K_0 by 8.4 %, LDA describing a too compressed structure with higher bulk modulus with respect to the experiment and PBE. The question can now be asked whether or not the choice of the adopted functional may affect the description of the temperature dependence of such structural properties. In order to investigate this point, Figure 3 reports the linear thermal expansion coefficient $\alpha_l(T)$ (upper panel), the volume of the primitive cell $V(T)$ (middle panel) and the bulk modulus $K(T)$ (lower panel) of diamond as a function of temperature. Computed values are reported as obtained with three different functionals, belonging to different families, of the DFT: LDA (thin continuous line), PBE (thick continuous line) and B3LYP (dashed line). Experimental data are also reported;[48,49,76,81] by comparing with them, it is seen that the temperature dependence of all quantities in the figure is quite well reproduced by all the functionals considered. In particular, this behavior is highlighted in the upper panel of the figure where $\alpha_l(T)$ is reported which is an entirely quasi-harmonic property. Differences among functionals can be observed which, however, are rather small if compared with those on harmonic properties such as V_0 and K_0. LDA provides a slightly lower thermal expansion than B3LYP and PBE. If one compares the equilibrium volumes at $T = 1600$ K (middle panel), as given by LDA and PBE, a difference of 3.7 % is found between the two with respect to 3.6 % at $T = 0$ K; the largest effect of the adopted functional on the temperature dependence of the equilibrium volume is then about only 0.1 %.

These findings are found to agree with the conclusions drawn by Narasimhan and De Gironcoli who discussed the relative performance of LDA and PBE functionals on describing the thermal expansion of bulk copper.[85] They also found that, at all temperatures, LDA was systematically underestimating the equilibrium volume and PBE overestimating it; the opposite behavior was reported for

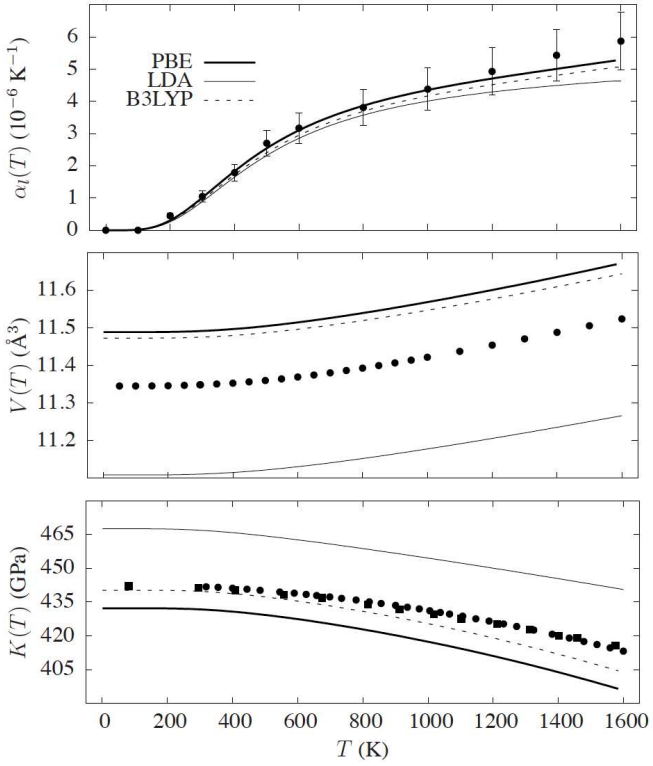

FIG. 3. Linear thermal expansion coefficient $\alpha_l(T)$, volume of the primitive cell $V(T)$ and bulk modulus $K(T)$ of diamond as a function of temperature. Computed values are reported as obtained with three different functionals of the DFT: LDA (thin continuous line), PBE (thick continuous line) and B3LYP (dashed line). Experimental data at room pressure for $\alpha_l(T)$ are from Slack and Bartram,[48] for $V(T)$ from Reeber and Wang[49] and for $K(T)$ from Zouboulis *et al.*[76] (full circles) and Aguado and Baonza[81] (full squares).

the bulk modulus as in the present study, as expected. The LDA prediction of thermal expansion was found to be lower than the PBE one, as here reported for diamond.

As illustrated in Section II B, Helmholtz's free energy approach allows for pressure and temperature effects on structural properties of materials to be combined together. The equilibrium volume of a crystal at a given temperature and pressure, $V(P,T)$, can be computed. To do so, the volume range to be explicitly explored has to be widened both as regards compression (for pressure) and expansion (for temperature). In particular, two kind of instructive representations can be given to the information embodied in $V(P,T)$: i) the equation of state (*i.e.* the pressure-volume relation) at different temperatures and ii) the thermal expansion coefficient at different pressures, $\alpha(T;P)$. Both quantities are reported in Figure 4 as computed with the PBE functional. On the left panel, experimental data at ambient pressure are by Slack and Bartram,[48] while, on the right panel, experimental data at room temperature are from Aleksandrov *et al.*[86] The linear expansion coefficient is reported at four different pressures: ambient, 4 GPa, 10 GPa and 20

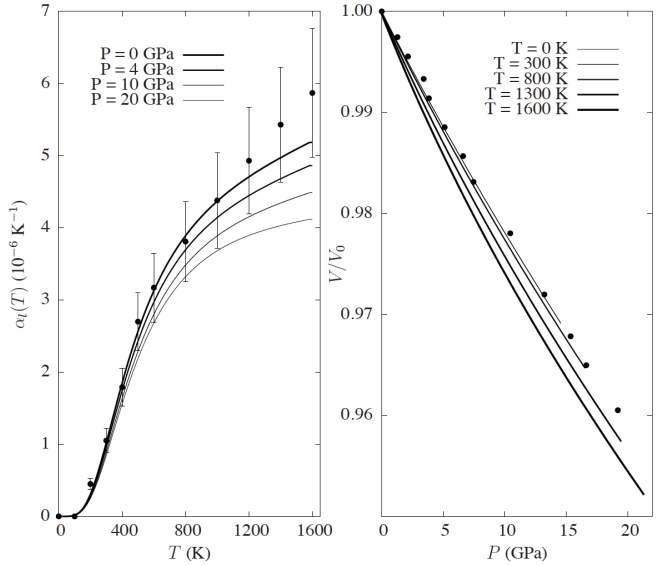

FIG. 4. (Left panel) linear thermal expansion $\alpha_l(T)$ of diamond as computed at different pressures. Experimental data at ambient pressure are by Slack and Bartram.[48] (Right panel) $V(P;T)/V_0(T)$ as a function of pressure for diamond, as computed at several temperatures. Experimental data at room temperature are from Aleksandrov *et al.*[86] All computed data are obtained with the PBE functional.

GPa. It is seen that $\alpha_l(T;P)$ is progressively reduced by pressure. The $V(P;T)/V_0(T)$ ratio, where $V_0(T)$ represents the equilibrium volume at temperature T and zero pressure, is reported on the right panel as a function of pressure for five different temperatures (T = 0, 300, 800, 1300 and 1600 K). The computed equation of state at 300 K is in relatively good agreement with experimental data at room temperature. As temperature increases, the compression of diamond induced by a given pressure increases.

V. CONCLUSIONS

A series of *ab initio* theoretical techniques, based on the DFT, for the combined study of temperature and pressure effects on structural properties of materials has been implemented, in a fully-automated fashion, into a development version of the public CRYSTAL14 program, taking advantage of its optimized algorithms for (massive) parallel calculations. Crystals of any space group can be treated by fully exploiting translation and point symmetry. The accurate determination of the thermal expansion coefficient requires the lattice dynamics of the crystal to be properly described; a direct-space supercell approach is adopted (convergence of computed properties on super-cell size has to be carefully checked). Anharmonic effects are included via the so-called quasi-harmonic approximation which introduces an explicit dependence of phonon frequencies on volume. The equilibrium structure at any temperature and pressure is obtained by minimizing Helmholtz's free energy.

These techniques are applied to the simple case of cubic diamond; theoretical results are compared with available experimental determinations. A super-cell containing 64 carbon atoms is shown to provide a satisfactory description of the thermal expansion of this crystal. The effect on computed structural properties of the particular approximation made in describing the exchange-correlation term of the electron-electron interaction is discussed into detail. Three different families of functionals are considered, which correspond to three different rungs of Perdew's "Jacob's ladder": a local-density approximation (LDA), a generalized-gradient approximation (GGA) and the hybrid B3LYP functional that is efficiently implemented in the CRYSTAL program. LDA is found to systematically underestimate the equilibrium volume and overestimate the bulk modulus. The opposite is true for GGA, even though at a smaller extent. B3LYP behaves similarly to GGA as regards volume but increases the agreement with the experiment on the bulk modulus. The temperature dependence of these properties is described very similarly by all functionals, LDA describing a slightly lower thermal expansion than B3LYP and GGA.

Further applications of this scheme are currently in progress to different families of crystals: simple ionic systems such as MgO, CaO, alkali halides, complex minerals of geophysical interest such as silicate garnets, BN monolayer and nanotubes.

[1] R. Dovesi, B. Civalleri, C. Roetti, V. R. Saunders, and R. Orlando, Rev. Comp. Chem. **21**, 1 (2005).
[2] S. Grimme, J. Antony, S. Ehrlich, and H. Krieg, J. Chem. Phys. **132**, 154104 (2010).
[3] C. Pisani, *Quantum-Mechanical Ab-initio Calculation of the Properties of Crystalline Materials*, vol. 67 of *Lecture Notes in Chemistry Series* (Springer Verlag, Berlin, 1996).
[4] R. Dronskowski, *Computational Chemistry of Solid State Materials* (Wiley, Weinheim, 2005).
[5] P. Ugliengo, M. Sodupe, F. Musso, I. J. Bush, R. Orlando, and R. Dovesi, Advanced Materials **20**, 4579 (2008).
[6] M. Delle Piane, M. Corno, and P. Ugliengo, J. Chem. Theor. Comput. **9**, 2404 (2013).
[7] E. Albanese, B. Civalleri, M. Ferrabone, F. Bonino, S. Galli, A. Maspero, and C. Pettinari, J. Mater. Chem. **22**, 22592 (2012).
[8] A. Erba, A. Mahmoud, R. Orlando, and R. Dovesi, Phys. Chem. Minerals **41**, 151 (2014).
[9] B. B. Karki, L. Stixrude, and R. M. Wentzcovitch, Rev. Geophys. **39**, 507 (2001).
[10] T. Barron, J. Collins, and G. White, Adv. Phys. **29**, 609 (1980).
[11] T. S. Koritsanszky and P. Coppens, Chem. Rev. **101**, 1583 (2001).
[12] F. D. Murnagham, Proc. Natl. Acad. Sci. USA **30**, 244 (1944).
[13] F. Birch, Phys. Rev. **71**, 809 (1947).
[14] F. Birch, J. Geophys. Res. **83**, 1257 (1978).
[15] J.-P. Poirier and A. Tarantola, Physics of the Earth and Planetary Interiors **109**, 1 (1998).
[16] P. Vinet, J. Ferrante, J. R. Smith, and J. H. Rose, J. Phys. C **19**, 467 (1986).
[17] I. Souza and J. Martins, Phys. Rev. B **55**, 8733 (1997).
[18] K. Doll, Molecular Physics **108**, 223 (2010).
[19] B. B. Karki, G. J. Ackland, and J. Crain, J. Phys.: Cond. Matter **9**, 8579 (1997).

[20] J. Wang, J. Li, S. Yip, S. Phillpot, and D. Wolf, Phys. Rev. B **52**, 12627 (1995).
[21] D. C. Wallace, *Thermodynamics of Crystals* (Wiley, New York, USA, 1972).
[22] D. C. Wallace, Rev. Mod. Phys. **37**, 57 (1965).
[23] A. Erba, A. Mahmoud, D. Belmonte, and R. Dovesi, J. Chem. Phys. **140**, 124703 (2014).
[24] A. Mahmoud, A. Erba, K. Doll, and R. Dovesi, J. Chem. Phys. **140**, 234703 (2014).
[25] A. G. Császár, C. Fábri, T. Szidarovszky, E. Mátyus, T. Furtenbacher, and G. Czakó, Phys. Chem. Chem. Phys. **14**, 1085 (2012).
[26] R. Car and M. Parrinello, Phys. Rev. Lett. **55**, 2471 (1985).
[27] F. Buda, R. Car, and M. Parrinello, Phys. Rev. B **41**, 1680 (1990).
[28] F. D. Vila, V. E. Lindahl, and J. J. Rehr, Phys. Rev. B **85**, 024303 (2012).
[29] K. N. Trueblood, H.-B. Bürgi, H. Burzlaff, J. D. Dunitz, C. M. Gramaccioli, H. H. Shulz, U. Shmueli, and C. Abrahams, Acta Cryst. A **52**, 770 (1996).
[30] A. Erba, M. Ferrabone, R. Orlando, and R. Dovesi, J. Comput. Chem. **34**, 346 (2013).
[31] A. O. Madsen, B. Civalleri, M. Ferrabone, F. Pascale, and A. Erba, Acta Crystallogr. Sec. A **69**, 309 (2013).
[32] Y. Sakurai, Y. Tanaka, A. Bansil, S. Kapzyk, A. T. Stewart, Y. Nagashima, T. Hyodo, S. Nanao, H. Kawata, and N. Shiotani, Phys. Rev. Lett. **74**, 2252 (1995).
[33] C. Blaas, J. Redinger, S. Manninen, V. Honkimäki, K. Hämäläinen, and P. Suortti, Phys. Rev. Lett. **75**, 1984 (1995).
[34] A. Erba, C. Pisani, S. Casassa, L. Maschio, M. Schütz, and D. Usvyat, Phys. Rev. B **81**, 165108 (2010).
[35] C. Pisani, M. Itou, Y. Sakurai, R. Yamaki, M. Ito, A. Erba, and L. Maschio, Phys. Chem. Chem. Phys. **13**, 933 (2011).
[36] A. Erba, M. Itou, Y. Sakurai, R. Yamaki, M. Ito, S. Casassa, L. Maschio, A. Terentjevs, and C. Pisani, Phys. Rev. B **83**, 125208 (2011).
[37] C. Pisani, A. Erba, S. Casassa, M. Itou, and Y. Sakurai, Phys. Rev. B **84**, 245102 (2011).
[38] S. B. Dugdale and T. Jarlborg, Solid State Commun. **105**, 283 (1998).
[39] C. Sternemann, G. Döring, C. Wittkop, W. Schülke, A. Shukla, T. Buslaps, and P. Suortti, J. Phys. Chem. Solids **61**, 379 (2000).
[40] C. Pisani, A. Erba, M. Ferrabone, and R. Dovesi, J. Chem. Phys. **137**, 044114 (2012).
[41] R. Orlando, M. Delle Piane, I. J. Bush, P. Ugliengo, M. Ferrabone, and R. Dovesi, J. Comput. Chem. **33**, 2276 (2012).
[42] R. Dovesi, R. Orlando, A. Erba, C. M. Zicovich-Wilson, B. Civalleri, S. Casassa, L. Maschio, M. Ferrabone, M. De la Pierre, P. D'Arco, et al., Int. J. Quantum Chem. **114**, 1287 (2014).
[43] N. W. Ashcroft and N. D. Mermin, *Solid State Physics* (Saunders College, Philadelphia, USA, 1976).
[44] S. Baroni, P. Giannozzi, and E. Isaev, Reviews in Mineralogy and Geochemistry **71**, 39 (2010).
[45] R. E. Allen and F. W. De Wette, Phys. Rev. **179**, 873 (1969).
[46] L. L. Boyer, Phys. Rev. Lett. **42**, 584 (1979).
[47] R. Dovesi, V. R. Saunders, C. Roetti, R. Orlando, C. M. Zicovich-Wilson, F. Pascale, K. Doll, N. M. Harrison, B. Civalleri, I. J. Bush, et al., *CRYSTAL14 User's Manual*, Università di Torino, Torino (2014), http://www.crystal.unito.it.
[48] G. A. Slack and S. F. Bartram, J. Appl. Phys. **46**, 89 (1975).
[49] R. R. Reeber and K. Wang, J. Elect. Mater. **25**, 63 (1996).
[50] T. Sato, K. Ohashi, T. Sudoh, K. Haruna, and H. Maeta, Phys. Rev. B **65**, 092102 (2002).
[51] C. H. Xu, C. Z. Wang, C. T. Chan, and K. M. Ho, Phys. Rev. B **43**, 5024 (1991).
[52] N. Mounet and N. Marzari, Phys. Rev. B **71**, 205214 (2005).
[53] P. Pavone, K. Karch, O. Schütt, D. Strauch, W. Windl, P. Giannozzi, and S. Baroni, Phys. Rev. B **48**, 3156 (1993).
[54] J. Xie, S. P. Chen, J. S. Tse, S. d. Gironcoli, and S. Baroni, Phys. Rev. B **60**, 9444 (1999).
[55] C. P. Herrero and R. Ramírez, Phys. Rev. B **63**, 024103 (2000).
[56] M. Prencipe, M. Bruno, F. Nestola, M. De La Pierre, and P. Nimis, Am. Mineral. **99**, 1147 (2014).
[57] F. Pascale, C. M. Zicovich-Wilson, R. Orlando, C. Roetti, P. Ugliengo, and R. Dovesi, J. Phys. Chem. B **109**, 6146 (2005).
[58] C. Carteret, M. De La Pierre, M. Dossot, F. Pascale, A. Erba, and R. Dovesi, J. Chem. Phys. **138**, 014201 (2013).
[59] A. Erba, S. Casassa, R. Dovesi, L. Maschio, and C. Pisani, J. Chem. Phys. **130**, 074505 (2009).
[60] M. Neff and G. Rauhut, J. Chem. Phys. **131**, 124129 (2009).
[61] J. O. Jung and R. B. Gerber, J. Chem. Phys. **105**, 10682 (1996).
[62] C. Lin, A. T. Gilbert, and P. M. Gill, Theor. Chem. Acc. **120**, 23 (2008).
[63] D. A. Broido, M. Malorny, G. Birner, N. Mingo, and D. A. Stewart, Applied Physics Letters **91**, 231922 (2007).
[64] D. Vanderbilt, S. H. Taole, and S. Narasimhan, Phys. Rev. B **40**, 5657 (1989).
[65] A. A. Maradudin, E. W. Montroll, and G. H. Weiss, *Theory of Lattice Dynamics in the Harmonic Approximation*, vol. 3 (Academic, New York, 1963).
[66] B. B. Karki, R. M. Wentzcovitch, S. de Gironcoli, and S. Baroni, Phys. Rev. B **61**, 8793 (2000).
[67] K. Doll, Comp. Phys. Comm. **137**, 74 (2001).
[68] K. Doll, N. M. Harrison, and V. R. Saunders, Int. J. Quantum Chem. **82**, 1 (2001).
[69] B. Civalleri, P. D'Arco, R. Orlando, V. R. Saunders, and R. Dovesi, Chem. Phys. Lett. **348**, 131 (2001).
[70] C. G. Broyden, IMA J. Appl. Math. **6**, 76 (1970).
[71] R. Fletcher, Comput. J. **13**, 317 (1970).
[72] D. Goldfarb, Mathematics of Computation **24**, 23 (1970).
[73] D. F. Shanno, Mathematics of Computation **24**, 647 (1970).
[74] F. Pascale, C. M. Zicovich-Wilson, F. L. Gejo, B. Civalleri, R. Orlando, and R. Dovesi, J. Comp. Chem. **25**, 888 (2004).
[75] C. M. Zicovich-Wilson, F. Pascale, C. Roetti, V. R. Saunders, R. Orlando, and R. Dovesi, J. Comp. Chem. **25**, 1873 (2004).
[76] E. S. Zouboulis, M. Grimsditch, A. K. Ramdas, and S. Rodriguez, Phys. Rev. B **57**, 2889 (1998).
[77] J. P. Perdew, K. Burke, and M. Ernzerhof, Phys. Rev. Lett. **77**, 3865 (1996).
[78] A. D. Becke, J. Chem. Phys. **88**, 2547 (1988).
[79] C. Lee, W. Yang, and R. G. Parr, Phys. Rev. B **37**, 785 (1988).
[80] M. F. Peintinger, D. V. Oliveira, and T. Bredow, J. Comput. Chem. **34**, 451 (2013).
[81] F. Aguado and V. G. Baonza, Phys. Rev. B **73**, 024111 (2006).
[82] O. Madelung, *Physics of Group IV and III-V Compounds*, vol. 17 (Springer-Verlag, Berlin, 1982).
[83] A. C. Victor, J. Chem. Phys. **36**, 1903 (1962).
[84] In the sampling of reciprocal space, for the primitive cell, a shrinking factor of 8 has been used which has been progressively reduced for conventional SCs as their size L has been increased: 3 for $L = 1$, 2 for $L = 2$ and 1 for $L = 3, 4, 5$. In all cases, these shrinking factor values correspond to a converged description of the electronic structure of the system.
[85] S. Narasimhan and S. de Gironcoli, Phys. Rev. B **65**, 064302 (2002).
[86] I. V. Aleksandrov, A. F. Goncharov, A. N. Zisman, and S. M. Stishov, Sov. Phys. JETP **66**, 384 (1987).